Alexandria Engineering Journal (2014) 53, 191–197

Alexandria University

Alexandria Engineering Journal

www.elsevier.com/locate/aej
www.sciencedirect.com

ORIGINAL ARTICLE

Numerical simulation of peristaltic flow of a Carreau nanofluid in an asymmetric channel

Noreen Sher Akbar [a,*], **S. Nadeem** [b], **Zafar Hayat Khan** [c]

[a] *DBS&H, CEME, National University of Sciences and Technology, Islamabad, Pakistan*
[b] *Department of Mathematics, Quaid-i-Azam University 45320, Islamabad 44000, Pakistan*
[c] *School of Mathematical Sciences, Peking University, Beijing 100871, PR China*

Received 22 August 2013; revised 12 October 2013; accepted 19 October 2013
Available online 22 November 2013

KEYWORDS

Peristaltic flow;
Nanofluid;
Carreau fluid model;
Asymmetric channel;
Fourth and fifth order Runge–Kutta–Fehlberg method

Abstract In this article, we studied MHD peristaltic flow of a Carreau nanofluid in an asymmetric channel. The flow development is carried out in a wave frame of reference moving with velocity of the wave c_1. The governing nonlinear partial differential equations are transformed into a system of coupled nonlinear ordinary differential equations using similarity transformations and then tackled numerically using the fourth and fifth order Runge–Kutta–Fehlberg. Numerical results are obtained for dimensionless velocity, stream function, pressure rise, temperature and nanoparticle volume fraction. It is found that the pressure rise increases with increase in Hartmann Number and thermophoresis parameter.

1. Introduction

Nanofluids are moderately new category of fluids which consist of a base fluid with nano-sized particles (1–100 nm) suspended within them. The term ''nanofluid'' was first proposed by Choi [1]on Argonne National Laboratory at 1995. He investigated that nanofluids reduced pumping power as compared to pure liquid to achieve equivalent heat transfer intensification and particle clogging as compared to conventional slurries, thus promoting system miniaturization. Xuan and Roetzel [2], analyzed theoretically the flow of a nanofluid inside a tube using a dispersion model. Heat transfer enhancement in a two-dimensional enclosure utilizing nanofluids is presented by Khanafer et al. [3] for various pertinent parameters. They developed model to analyze heat transfer performance of nanofluids inside an enclosure taking into account the solid particle dispersion. Review of convective heat transfer enhancement with nanofluids is given by Sadik and Pramuanjaroenkij [4]. The literature survey of Sadik and Pramuanjaroenkij [4] shows that nanofluids significantly improve the heat transfer capability of conventional heat transfer fluids such as oil or water by suspending nanoparticles in these base liquids. In the peristaltic literature nanofluid was first introduced by Nadeem and Akbar [5]. They discussed endoscopic effects on the peristaltic flow of a nanofluid. They made the analysis in two concentric tubes and discussed the applications of endoscope. Recent articles on the nanofluids are cited in Refs. [6–11].

* Corresponding author. Tel.: +92 05190642182.
E-mail address: noreensher@yahoo.com (N.S. Akbar).
Peer review under responsibility of Faculty of Engineering, Alexandria University.

Production and hosting by Elsevier

1110-0168 © 2013 Production and hosting by Elsevier B.V. on behalf of Faculty of Engineering, Alexandria University.
http://dx.doi.org/10.1016/j.aej.2013.10.003

Peristalsis is a mechanism of fluid flowing by means of moving contraction on the tubes/channels walls. This analysis was first discussed by Latham [12]. He presented fluid motion in peristaltic pump. He also discussed the characteristic of pressure rise versus flow rate. After the pioneering work of Latham [12], Jaffrin and Shapiro [13] investigated the peristaltic pumping. They made the analysis under the assumption of long wave length and low Reynolds number approximations. Later on a number of analytical, numerical and experimental studies of peristaltic flows of different fluids have been reported under different conditions with reference to physiological and mechanical situations. Peristaltic pumping by a sinusoidal traveling wave in the porous walls of a two-dimensional channel filled with a viscous incompressible conducting fluid under the effect of transverse magnetic field is investigated theoretically and graphically by El-Shehawey and Husseny [14]. Non-linear peristaltic transport of a Newtonian fluid in an inclined asymmetric channel through a porous medium is examined by Kothandapani and Srinivas [15]. In another article Srinivas and Kothandapani [16]. investigated the effects of heat and mass transfer on peristaltic transport in a porous space with compliant walls. They considered that fluid is electrically conducting in the presence of a uniform magnetic field and developed analytical solution under long-wavelength and low-Reynolds number approximations. Haroun [17], Mekheimer [18] and Nadeem and Akbar [19,20] coated the peristaltic flow phenomena in different geometries for different fluid models. Some more relevant article related to the topic are cited in Refs. [21–25].

The aim of the current study is to discuss the peristaltic flow of Carreau nanofluid in an asymmetric channel. The study of Carreau nanomodel for peristaltic flow problems is not explored so far. Therefore, to fill this gape in the present analysis we have discussed the peristaltic flow of Carreau fluid model with nanoparticle phenomena in an asymmetric channel. The article presentation is carried out as follows. Next section describes the mathematical formulation of the problem. Numerical solution graphically and in tabulated form for velocity, pressure rise, temperature, nanoparticle phenomena and streamlines have been presented in section three. Conclusion of the present work is presented in the last section of the article.

2. Mathematical formulation

Let us discussed an incompressible Carreau fluid with nanoparticle in an asymmetric channel of width $d_1 + d_2$. The channel has a sinusoidal wave propagating with constant speed c_1 on the channel walls induces the flow. The asymmetric of the channel is due to different amplitudes. Temperature $\overline{T}_0, \overline{T}_1$ and nanoparticle concentrations $\overline{C}_0, \overline{C}_1$ are given to the upper and lower wall of the channel. The wall surfaces are selected to satisfy the following expressions

$$Y = H_1 = d_1 + a_1 \cos\left[\frac{2\pi}{\lambda}(X - ct)\right],$$
$$Y = H_2 = -d_2 - b_1 \cos\left[\frac{2\pi}{\lambda}(X - ct) + \phi\right]. \quad (1)$$

In the above equations a_1 and b_1 are the waves amplitudes, λ is the wave length, $d_1 + d_2$ is the channel width, c_1 is the wave speed, t is the time, X is the direction of wave propagation and Y is perpendicular to X. The phase difference ϕ varies in the range $0 \leqslant \phi \leqslant \pi$. When $\phi = 0$ then symmetric channel with waves out of phase can be described and for $\phi = \pi$, the waves are in phase. Moreover, a_1, b_1, d_1, d_2 and ϕ satisfies the following relation

$$a_1^2 + b_1^2 + 2a_1 b_1 \cos\phi \leqslant (d_1 + d_2)^2.$$

The coordinates, velocity components and pressure between fixed and wave frames are related by the following transformations:

$$\bar{x} = \overline{X} - c_1 t,\ \bar{y} = \overline{Y},\ \bar{u} = \overline{U} - c_1,\ \bar{v} = \overline{V},\ p(\bar{x}) = P(\overline{X}, t), \quad (2)$$

in which $(\bar{x}, \bar{y}), (\bar{u}, \bar{v})$ and $\bar{p}$ are the coordinates, velocity components and pressure in the wave frame.

The constitutive equation for Carreau fluid is given by [19]

$$\frac{(\eta - \eta_\infty)}{(\eta_0 - \eta_\infty)} = \left[1 + \left(\Gamma\bar{\dot{\gamma}}\right)^2\right]^{\frac{(n-1)}{2}}, \quad (3a)$$

$$\bar{\tau}_{ij} = \eta_0\left[1 + \frac{(n-1)}{2}\left(\Gamma\bar{\dot{\gamma}}\right)^2\right]\bar{\dot{\gamma}}_{ij}, \quad (3b)$$

in which $\bar{\tau}_{ij}$ is the extra stress tensor, η_∞ is the infinite shear rate viscosity, η_0 is the zero shear rate viscosity, Γ is the time constant, n is the Power law index and $\dot{\gamma}$ is defined as

$$\bar{\dot{\gamma}} = \sqrt{\frac{1}{2}\sum_i\sum_j \bar{\dot{\gamma}}_{ij}\bar{\dot{\gamma}}_{ji}} = \sqrt{\frac{1}{2}\Pi}. \quad (3c)$$

Here Π is the second invariant strain tensor.

Velocity stream function relation and nondimensional quantities are

$$u = \frac{\partial\Psi}{\partial y},\ v = -\delta\frac{\partial\Psi}{\partial x}, \quad (4)$$

$$x = \frac{2\pi\bar{x}}{\lambda},\ y = \frac{\bar{y}}{d_1},\ u = \frac{\bar{u}}{c_1},\ v = \frac{\bar{v}}{c_1},\ t = \frac{2\pi\bar{t}}{\lambda},\ \delta = \frac{2\pi d_1}{\lambda},$$
$$d = \frac{d_2}{d_1},\ P = \frac{2\pi d_1^2 P}{\mu c_1\lambda}, h_1 = \frac{\bar{h}_1}{d_1},\ h_2 = \frac{\bar{h}_2}{d_2},\ \mathrm{Re} = \frac{\rho c_1 d_1}{\mu},\ a = \frac{a_1}{d_1},$$
$$b = \frac{a_2}{d_1},\ d = \frac{d_2}{d_1},\ S = \frac{\overline{S}d_1}{\mu c_1},\ We = \frac{\Gamma c}{a_2},\ \theta = \frac{\overline{T} - \overline{T}_0}{\overline{T}_1 - \overline{T}_0},$$
$$\sigma = \frac{\overline{C} - \overline{C}_0}{\overline{C}_1 - \overline{C}_0},\ \alpha = \frac{k}{(\rho c)_f},\ N_b = \frac{(\rho c)_p D_B(\overline{C}_1 - \overline{C}_0)}{(\rho c)_f\nu},\ P_r = \frac{\nu}{\alpha},$$
$$N_t = \frac{(\rho c)_p D_{\overline{T}}(\overline{T}_1 - \overline{T}_0)^2}{\overline{T}_0(\rho c)_f\nu},\ G_r = \frac{g\alpha d_1^2(\overline{T}_1 - \overline{T}_0)}{\nu c_1},$$
$$B_r = \frac{g\alpha d_1^2(\overline{C}_1 - \overline{C}_0)}{\nu c_1}. \quad (5)$$

Using Eqs. 2, 3, 4, 5, 6 after using the long-wavelength and low-Reynold's number approximation, we finally obtain the following system of equations for Carreau nanofluid.

$$\frac{\partial^2}{\partial y^2}\left[\frac{\partial^2\Psi}{\partial y^2} + \frac{(n-1)}{2}We^2\left(\frac{\partial^2\Psi}{\partial y^2}\right)^3 - M^2\Psi\right] + G_r\frac{\partial\theta}{\partial y} + B_r\frac{\partial\sigma}{\partial y} = 0, \quad (6)$$

$$\frac{dP}{dx} = \frac{\partial}{\partial y}\left[\frac{\partial^2\Psi}{\partial y^2} + \frac{(n-1)}{2}We^2\left(\frac{\partial^2\Psi}{\partial y^2}\right)^3 - M^2\Psi\right] + G_r\theta + B_r\sigma, \quad (7)$$

$$0 = \frac{\partial^2\theta}{\partial y^2} + \mathrm{Pr}N_b\frac{\partial\sigma}{\partial y}\frac{\partial\theta}{\partial y} + \mathrm{Pr}N_t\left(\frac{\partial\theta}{\partial y}\right)^2, \quad (8)$$

$$0 = \left(\frac{\partial^2 \sigma}{\partial y^2}\right) + \frac{N_t}{N_b}\left(\frac{\partial^2 \theta}{\partial y^2}\right). \tag{9}$$

where P_r the Prandtl number, We is the Weissenberg number, N_b the Brownian motion parameter, N_t the thermophoresis parameter, G_r the local temperature Grashof number, M the Hartmann number, B_r local nanoparticle Grashof number.

Corresponding boundary conditions for asymmetric channel in nondimensional form take the following form

$$\Psi = \frac{F}{2},\ \frac{\partial \Psi}{\partial y} = -1,\ \text{at } y = h_1 = 1 + a\cos x, \tag{10a}$$

$$\Psi = -\frac{F}{2},\ \frac{\partial \Psi}{\partial y} = -1,\ \text{at } y = h_2 = -d - b\cos(x+\phi), \tag{10b}$$

$$\theta = 0,\ \sigma = 0,\ y = h_1 = 1 + a\cos x, \tag{10c}$$

$$\theta = 1,\ \sigma = 1,\ y = h_2 = -d - b\cos(x+\phi) \tag{10d}$$

The time mean Q (in the wave frame) are defined as

$$Q = F + 1 + d. \tag{11}$$

The dimensionless pressure rise ΔP is defined as

$$\Delta P = \int_0^1 \left(\frac{dP}{dx}\right) dx. \tag{12}$$

3. Results and discussion

We have examined the pressure rise, pressure gradient, velocity, temperature, nanoparticle phenomena and streamlines for Carreau nanofluid model numerically. In order to analyze the pressure rise per wavelength the pressure rise against volume flow rate is portrayed in Fig. 1(a–f). It is observed that the

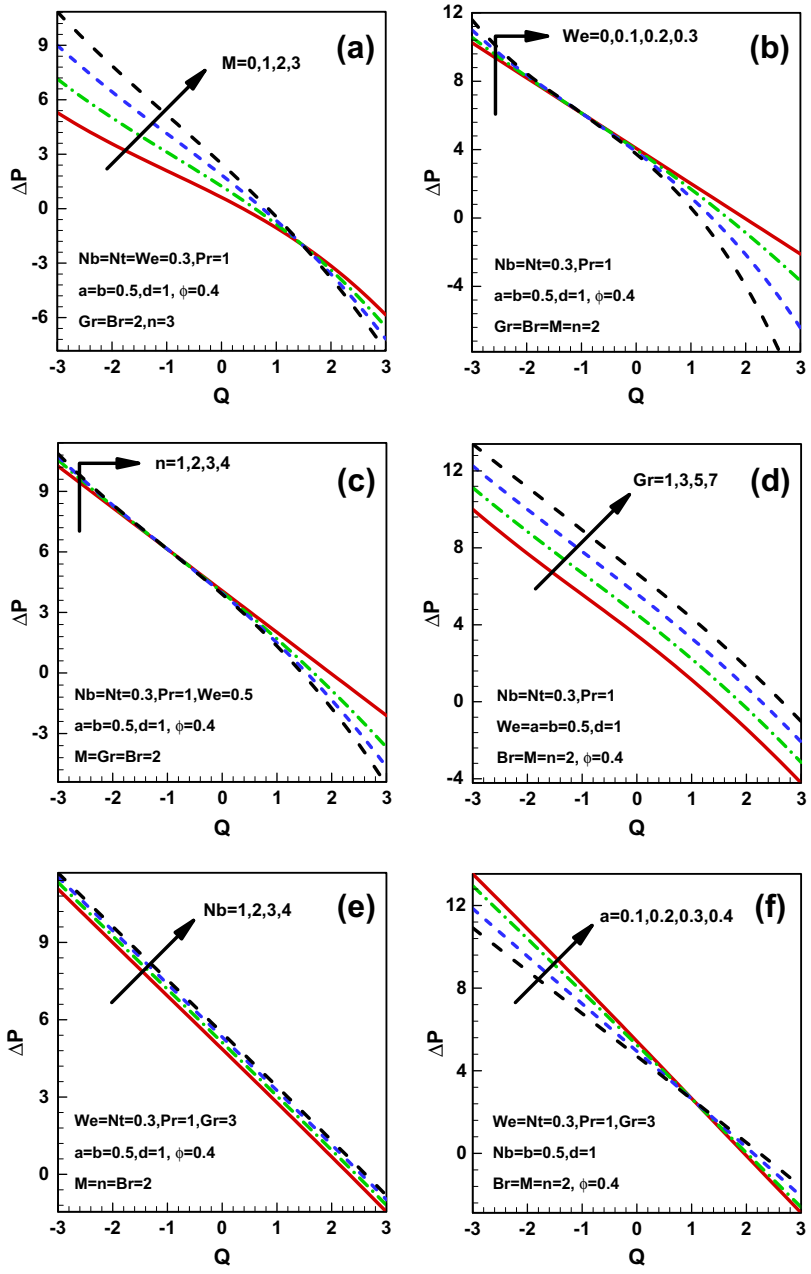

Figure 1 (a–f) Pressure rise versus flow rate.

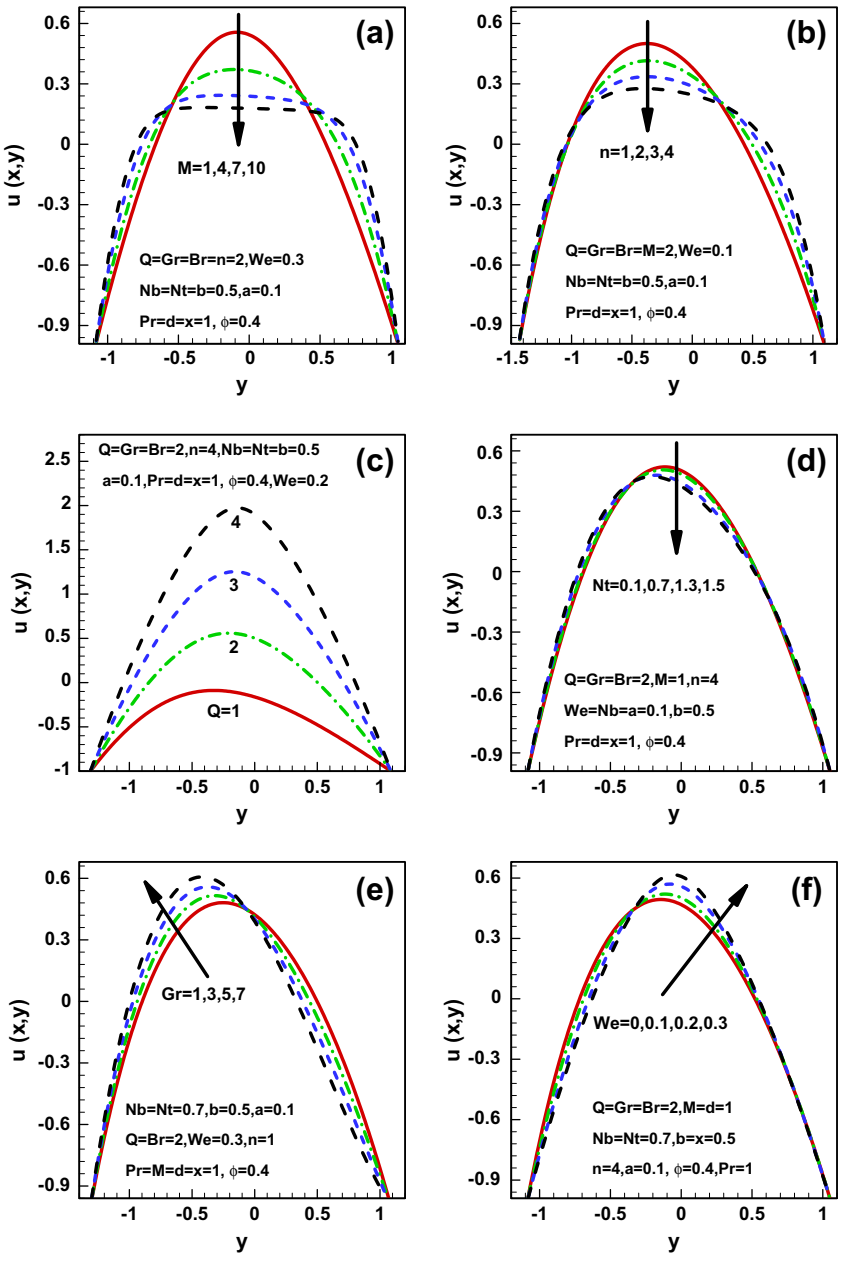

Figure 2 (a–f) Velocity profile.

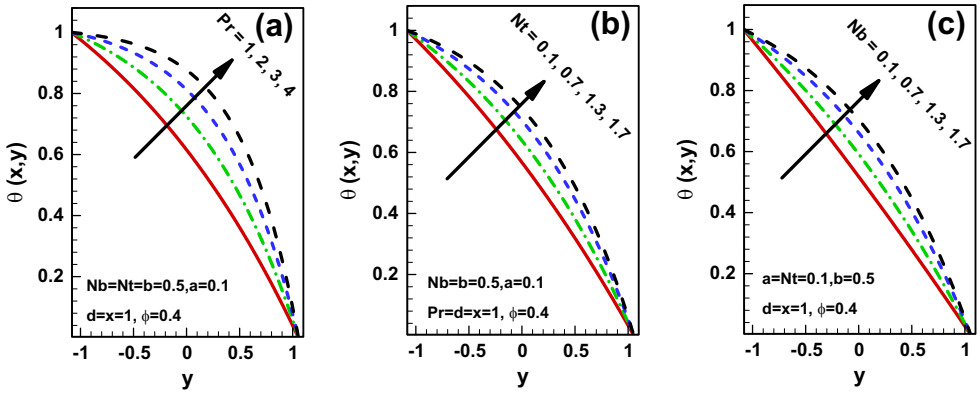

Figure 3 (a–c) Temperature profile.

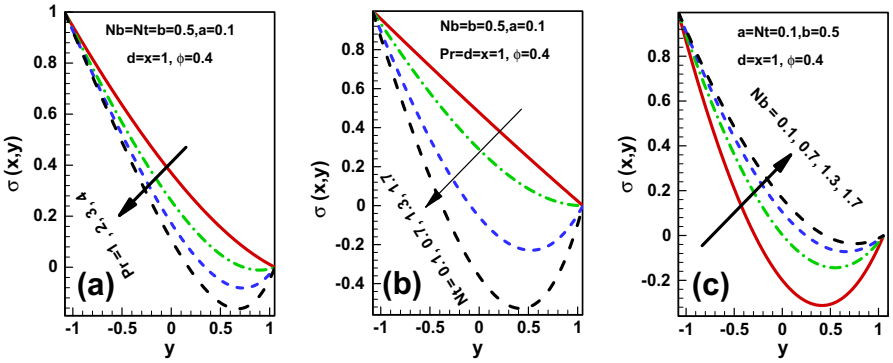

Figure 4 (a–c) Nano particle profile.

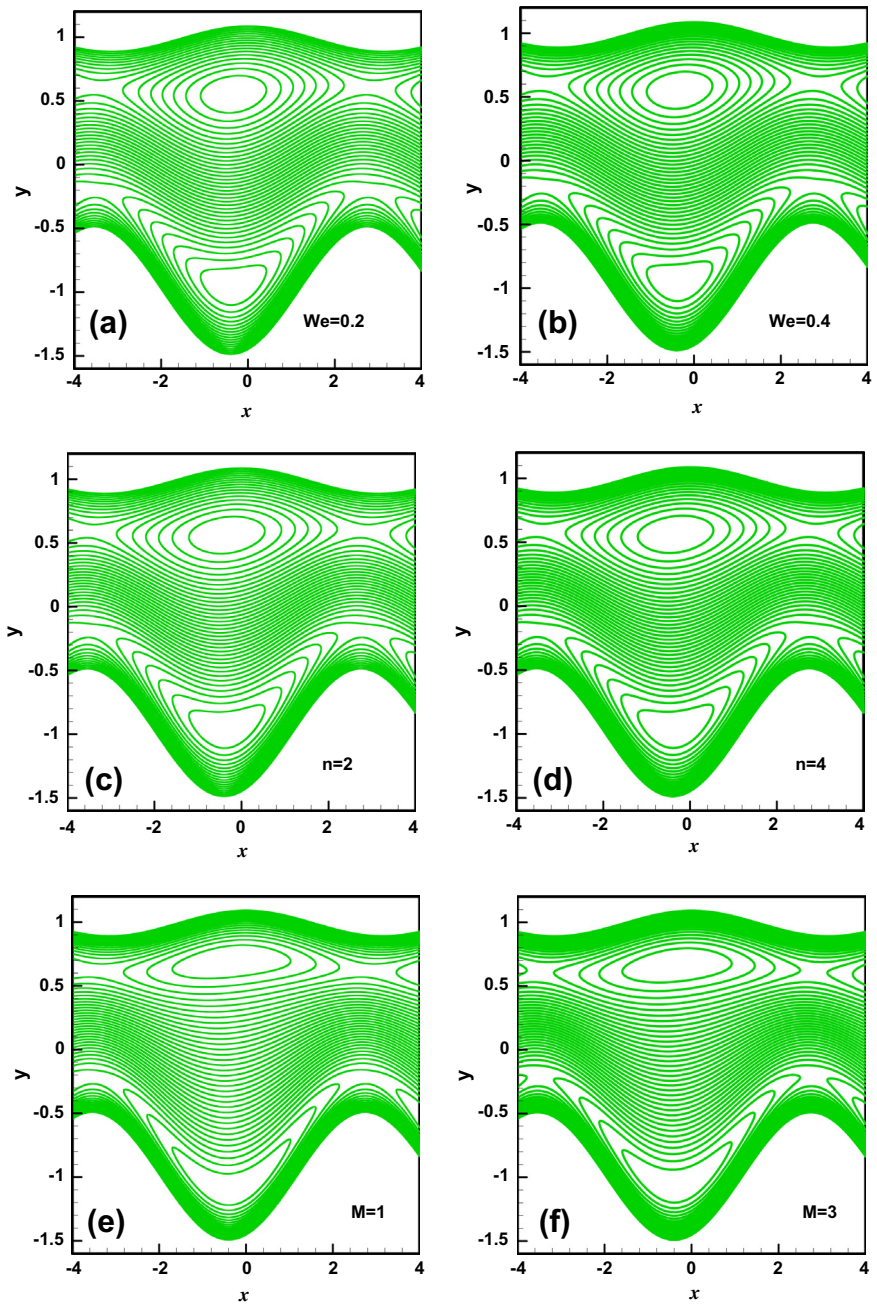

Figure 5 Streamlines for $a = 0.5, b = 0.5, d = 1, \phi = 0.4, G_r = 2, B_r = 2, Nb = 0.5, Nt = 0.5, K = 1, Pr = 1$.

Table 1 Numerical values of velocity profile for $x = 1, a = 0.1, d = 1, Nb = 0.5, Nt = 0.5, Br = 1, Gr = 5, M = 2, Q = 2, \phi = 0.4, We = 0.2, b = 0.5, n = 2$.

$\downarrow y$	$u(x, y)$	$\downarrow y$	$u(x, y)$	$\downarrow y$	$u(x, y)$
−1.10	−1.00000	−0.39	0.41064	0.39	0.16781
−1.00	−0.70803	−0.29	0.46499	0.49	0.04238
−0.89	−0.38724	−0.19	0.49067	0.59	−0.10135
−0.79	−0.14664	−0.09	0.48981	0.69	−0.26296
−0.69	0.04980	0.09	0.42715	0.89	−0.63894
−0.59	0.20594	0.19	0.36109	0.99	−0.85334
−0.49	0.32519	0.29	0.27432	1.10	−1.00000

Table 2 Numerical values of pressure rise ΔP for $a = 0.5, \Pr = 1, d = 1, Nb = 0.5, Nt = 0.5, Br = 2, Gr = 2, M = 2, \phi = 0.4, b = 0.5, n = 2, We = 1.5$.

$\downarrow Q$	ΔP	$\downarrow Q$	ΔP	$\downarrow Q$	ΔP
−3.0	11.59503	−1.0	6.13636	1.0	0.597007
−2.5	9.87075	−0.5	4.97221	1.5	−1.46174
−2.0	8.45405	0.0	3.74410	2.5	−7.02264
−1.5	7.26583	0.5	2.30386	3.0	−10.7076

pressure rise and volume flow rate are giving opposite behavior. From Fig. 1(a–f) it is also noticed that in pumping region ($\Delta P > 0$), the pressure rise increases with increase in Hartmann number M, Power law index n, Weisenberg number We, the thermophoresis parameter N_t, temperature Grashof number Gr and amplitude ratio a. Fig. 1(a–f) also show that in the augmented pumping region for ($\Delta P < 0$), the pressure decreases when Hartmann number M, Power law index n, Weisenberg number We, the thermophoresis parameter N_t, temperature Grashof number Gr and amplitude ratio a are increased. Free pumping region holds when ($\Delta P = 0$). Variations of Hartmann number M, Power law index n, Weisenberg number We, flow rate Q, local temperature Grashof number G_r and thermophoresis parameter N_t on the velocity profile are shown in Fig. 2(a–f). Fig. 2(a and b) depicts that the behavior of velocity near the channel walls and at center is not similar in view of the Hartmann number M and Power law index n. The velocity field increases with the increase in M and n near the channel walls however it decreases in the center of the channel. Velocity field increases with an increase in flow rate Q (see Fig. 2(c)). Fig. 2(d) depicts that by increasing N_t velocity field increases in the region $y \in [-1.5, 0]$ and decreases in rest of the region $y \in [0.1, 1.1]$. It is observed through Fig. 2(e) that by increasing G_r velocity field increases in the region $y \in [-1.5, 0]$ and decreases otherwise in the region $y \in [0.1, 1.1]$. Velocity field decreases in the region $y \in [-1.5, 0]$ and increases otherwise in the region $y \in [0.1, 1.1]$ when the value of Weisenberg number We increases.

The variation of temperature profile and nanoparticle concentration for different values of thermophoresis parameter N_t Prandtl parameter P_r and Brownian motion parameter N_b are plotted in Figs. 3 and 4. Here the temperature profile increases when thermophoresis parameter N_t, Prandtl parameter P_r and Brownian motion parameter N_b are increased and nanoparticle concentration decreases when there is an increase in the values of thermophoresis parameter N_t, Prandtl parameter P_r and increases with an increase in Brownian motion parameter N_b.

The trapping for different values of We, n and M is shown in Fig. 5(a–f). It is seen from Fig. 5(a and b) that the size of the trapping bolus decreases with an decrease in We (in the upper and lower part of the channel). Fig. 5(c and d) shows that the size of trapping bolus increases with an decrease in n in the upper and lower parts of the channel. Influence of M on streamlines is shown through Fig. 5(e and f), it is observed that with the increase in M size of trapping bolus decreases but number of bolus increases. Tables 1 and 2 gives the numerical values for velocity profile and pressure rise.

4. Concluding remarks

The present study discussed the MHD peristaltic flow of a Carreau nanofluid in an asymmetric channel. The main points of the current analysis are as follows:

1. The qualitative behaviors of Hartmann number M, Power law index n, Weisenberg number We, the thermophoresis parameter N_t, temperature Grashof number Gr and amplitude ratio a on the pressure rise are same.
2. The pressure rise increases with the increase of Hartmann number M, Power law index n, Weisenberg number We, the thermophoresis parameter N_t, temperature Grashof number Gr and amplitude ratio a.
3. The behavior of velocity near the channel walls and at center is not similar in view of the Hartmann number M and Power law index n.
4. The velocity field increases with the increase in M and n near the channel walls however it decreases in the center of the channel.
5. Velocity field increases with an increase in flow rate Q.
6. The temperature profile increases when thermophoresis parameter N_t, prandtl parameter P_r and Brownian motion parameter N_b are increased.

7. Nanoparticle phenomena decreases when there is an increase in the values of thermophoresis parameter N_t, prandtl parameter P_r and increases with an increase in Brownian motion parameter N_b.
8. Temperature profile increases with an increase in N_t and N_b.
9. Nanoparticle phenomena decreases with in N_t and increases with increase in N_b.
10. The size of the trapping bolus decreases with the decrease in We (in the upper and lower part of the channel).
11. The size of trapping bolus increases with the decrease in n in the upper and lower parts of the channel
12. It is observed that with the increase in M size of trapping bolus decreases but number of bolus increases.

References

[1] S.U.S. Choi, Enhancing thermal conductivity of fluids with nanoparticles, in: D.A. Siginer, H.P. Wang (Eds.), Developments and Applications of Non-Newtonian Flows, 66, ASME, New York, 1995, pp. 99–105.

[2] Y. Xuan, W. Roetzel, Conceptions for heat transfer correlation of nanofluids, Int. J. Heat Mass Transfer 43 (2000) 3701–3707.

[3] K. Khanafer, K. Vafai, M. Lightstone, Buoyancy-driven heat transfer enhancement in a two-dimensional enclosure utilizing nanofluids, Int. J. Heat Mass Transfer 46 (2003) 3639–3653.

[4] K. Sadik, A. Pramuanjaroenkij, Review of convective heat transfer enhancement with nanofluids, Int. J. Heat Mass Transfer 52 (2009) 3187–3196.

[5] Noreen Sher Akbar, S. Nadeem, Endoscopic effects on the peristaltic flow of a nanofluid, Commun. Theor. Phys. 56 (2011) 761–768.

[6] O.A. B ég, D. Tripathi, Mathematica simulation of peristaltic pumping with double-diffusive convection in nanofluids: a bio-nano-engineering model, J. Nanoeng. Nanosyst. (2012), http://dx.doi.org/10.1177/1740349912437087.

[7] A. Ebaid, E.H. Aly, Exact analytical solution of the peristaltic nanofluids flow in an asymmetric channel with flexible walls and slip condition: application to the cancer treatment, Comput. Math. Meth. Med. (2013) 8, http://dx.doi.org/10.1155/2013/825376 (Article ID 825376).

[8] M.A.A. Hamad, M. Ferdows, Similarity solution of boundary layer stagnation-point flow towards a heated porous stretching sheet saturated with a nanofluid with heat absorption/generation and suction/blowing: a lie group analysis, Commun. Nonlinear Sci. Numer. Simul. 17 (2012) 132–140.

[9] Noreen Sher Akbar, S. Nadeem, T. Hayat, Awatif A Hendi, Peristaltic flow of a nano fluid with slip effects, Meccanica 47 (2012) 1283–1294.

[10] Noreen Sher Akbar, S. Nadeem, T. Hayat, Awatif A Hendi, Peristaltic flow of a nanofluid in a non-uniform tube, Heat Mass Transfer 48 (2012) 451–459.

[11] Noreen Sher Akbar, S. Nadeem, Peristaltic flow of a Phan-Thien–Tanner nanofluid in a diverging tube, Heat Transfer Res. 41 (2012) 10–22.

[12] T.W. Latham, Fluid Motion in a Peristaltic Pump, MS. Thesis, Massachusetts Institute of Technology, Cambridge, 1966.

[13] M Y Jaffrin, A H Shapiro, Peristaltic pumping, Ann. Rev. Fluid Mech. 37 (1971) 13–37.

[14] E.F. El-Shehawey, Saleh Z.A. Husseny, Peristaltic transport of a magneto-fluid with porous boundaries, Appl. Math. Comput. 129 (2002) 421–440.

[15] M. Kothandapani, S. Srinivas, Non-linear peristaltic transport of a Newtonian fluid in an inclined asymmetric channel through a porous medium, Phys. Lett. A 372 (2008) 1265–1276.

[16] S. Srinivas, M. Kothandapani, The influence of heat and mass transfer on MHD peristaltic flow through a porous space with compliant walls, Appl. Math. Comput. 213 (2009) 197–208.

[17] M.H. Haroun, Non-linear peristaltic flow of a fourth grade fluid in an inclined asymmetric channel, Comput. Mater. Sci. 39 (2007) 324–333.

[18] Kh. S. Mekheimer, Effect of the induced magnetic field on peristaltic flow of a couple stress fluid, Phys. Lett. A 372 (2008) 4271–4278.

[19] S. Nadeem, Noreen Sher Akbar, Effects of heat and mass transfer on peristaltic flow of Carreau fluid in a vertical annulus, Z. Naturforsc. 65a (2010) 781–792.

[20] Noreen Sher Akbar, S. Nadeem, Thermal and velocity slip effects on the peristaltic flow of a six constant Jeffrey's fluid model, Int. J. Heat Mass Transfer 55 (2012) 3964–3970.

[21] R. Ellahi, A. Riaz, Analytical solution for MHD flow in a third grade fluid with variable viscosity, Math. Comput. Model. 52 (2010) 1783–1793.

[22] M. Hameed, R. Ellahi, Thin film flow of non-Newtonian MHD fluid on a vertically moving belt, Int. J. Numer. Method Fluids 66 (11) (2011) 1409–1419.

[23] M. Hameed, R. Ellahi, Numerical and analytical solutions of an Oldroyd 8-constant MHD fluid with nonlinear slip conditions, Int. J. Numer. Method Fluids 67 (10) (2011) 1234–1246.

[24] R. Ellahi, A. Zeeshan, K. Vafai, H.U. Rahman, Series solutions for magnetohydrodynamic flow of non-Newtonian nanofluid and heat transfer in coaxial porous cylinder with slip conditions, J. Nanoeng. Nanosyst. 225 (3) (2011) 123–132.

[25] Noreen Sher Akbar, S. Nadeem, C. Lee, Z.H. Khan, R. Haq, Numerical study of Williamson nano fluid flow in an asymmetric channel, Results Phys. 3 (2013) 161–166.